THE ARCHIVE OF MECHANICAL ENGINEERING

VOL. LVI 2009 Number 1

DOI: 10.24425/ame.2009.132085

Key words: compression ignition engine, modelling, optimization, emission control

KRZYSZTOF BRZOZOWSKI *, *JACEK NOWAKOWSKI* **

THE APPLICATION OF OPTIMIZATION METHOD TO CONTROL CI ENGINE EXHAUST EMISSION UNDER STEADY-STATE CONDITIONS

In this paper, the semi-empirical model, formulated in the earlier paper [1], was used to control engine exhaust emission under steady-state conditions. The presented optimization method enables us to find the values of engine control parameters that lead to minimization of nitrogen oxide emission. Moreover, the presented method ensures proper engine operating parameters such as mean indicated pressure, thermal efficiency and maximum pressure in the cylinder. Results of numerical calculations are compared with experiment data. An acceptable accuracy was achieved.

NOTATION

B_0	–	injected fuel mass,
$\boldsymbol{E}$	–	vector of model parameters.
f_s	–	approximate value,
k_h	–	coefficient in the Hohenberg formula,
m_c	–	mass of the medium in the cylinder,
m_d	–	mass of the medium in the intake manifold,
m_w	–	mass of the medium in the exhaust manifold,
m_v	–	Vibe constant,
$M_{\max}$	–	maximum torque of an engine,

* *University of Bielsko-Biała, Department of Mechanics and Computer Science, Willowa 2, Bielsko-Biała 43-309, Poland; E-mail: kbrzozowski@ath.eu*

** *University of Bielsko-Biała, Department of Combustion Engines and Vehicles, Willowa 2, Bielsko-Biała 43-309, Poland; E-mail: jnowakow@ath.eu*

n	–	crankshaft rotational speed,
p_c	–	cylinder pressure,
p_d	–	intake manifold pressure,
p_w	–	exhaust manifold pressure,
p_i	–	indicated mean pressure in the cylinder,
$p_{\max}$	–	maximum cylinder pressure,
T_c	–	cylinder temperature,
T_d	–	temperature in the intake manifold,
T_w	–	temperature in the exhaust manifold,
$T_{\max}$	–	maximum cylinder temperature,
t	–	time,
V	–	volume,
V_c	–	cylinder volume,
$\boldsymbol{X}$	–	vector of control parameters,
X_{EGR}	–	degree of exhaust gas recirculation,
δ_i^s	–	coefficient in an approximating function,
η_c	–	thermal efficiency,
φ	–	crank angle,
φ_z	–	start of combustion,
$\Delta\varphi_s$	–	total combustion duration,
φ_w	–	injection advance angle,
μ_d	–	inlet valve discharge coefficient,
μ_w	–	exhaust valve discharge coefficient.

1. Introduction

The phenomena occurring in the engine cylinder can be described by a set of partial differential equations [2]; however, the complex CFD models require long computational time and their use in optimization of the emissions is limited. Thus a simple and numerically effective semi-empirical model is often used.

The engine cylinder and the intake and exhaust manifolds can be treated as an open thermodynamic system. The equations of mass and energy conservation are used to describe phenomena in the cylinder, and they are written for an independent variable like time or crank angle. Models of intake and exhaust manifolds describe the flow in the manifold systems. In practice, three different types of models are used in order to model the intake and the exhaust flows:

– quasi-steady model, in which valves, ports and other elements are taken into account,
– filling and emptying model, for which the concept of the finite volume of manifolds is used,
– gas dynamic model based on unsteady flow throughout the manifolds, which is described by wave equations.

In the quasi-steady model, the manifolds are considered as a series of interconnected components. Each component, such as air cleaner, throttle, port or valves, constitutes a significant flow restriction. Geometrical dimensions and discharge coefficients are used to model the flow over them. As a result, the gas flow rate is computed from one dimensional flow equation. The quasi-steady models are often used to calculate the flow into and out of the cylinder through the inlet and exhaust valves. This approach was used in the paper [1] for engine cycle simulation.

The single-zone models are often used in order to calculate thermodynamic parameters in the cylinder. One or more algebraic equations are used to describe an averaged thermodynamic properties of the medium. Coefficients in equations are chosen to match experimentally observed heat release profiles. They are dependent on design details and operating conditions of the engine. There are many different equations proposed by Vibe, Watson, Whitehouse and Way [3–6]. Watson and Vibe equations are most commonly used for CI engine modelling. The Watson equation describes two phases of the combustion process in a direct injection diesel engine. The Vibe equation is much simpler than Watson equation, because only one parameter is unknown and has to be derived experimentally [7].

The earlier paper [1] presented the application of optimization methods to determine the parameters of the numerical model using the experimental measurements taken for a given set of control engine parameters. In order to obtain the estimated parameters of the model (valve discharge coefficients, heat transfer and Vibe function parameters) for a set of control parameters the approximation task has been formulated and solved.

The paper shows how the model (after the calibration process) can be used for choosing such engine control parameters that would ensure reduction or minimization of the emission of nitrogen oxides. This problem is also formulated as an optimization task on the basis of the calibrated model and the results of measurements. This approach differs significantly from the methodology generally used in other research, such as the multi-zone combustion model for predicting nitrogen oxide emission [8–13] or experimental prediction of parameters of a variable geometry turbine VGT/EGR or multiple-injection [14–17]. In this paper, the appropriate optimization tasks were formulated and carried out in order to find the minimum emission of nitrogen oxides. Additional boundary conditions for other exhaust gas components, mean effective pressure, thermal efficiency and maximum pressure in the cylinder are taken into account in the proposed procedure.

Figure 1 shows the general algorithm applied in the formulation of the computational model of the working cycle of the CI engine used in our study. The algorithm is divided into two steps: the first for obtaining the calibrated model presented in [1] and the second for solving emission control tasks presented in this paper.

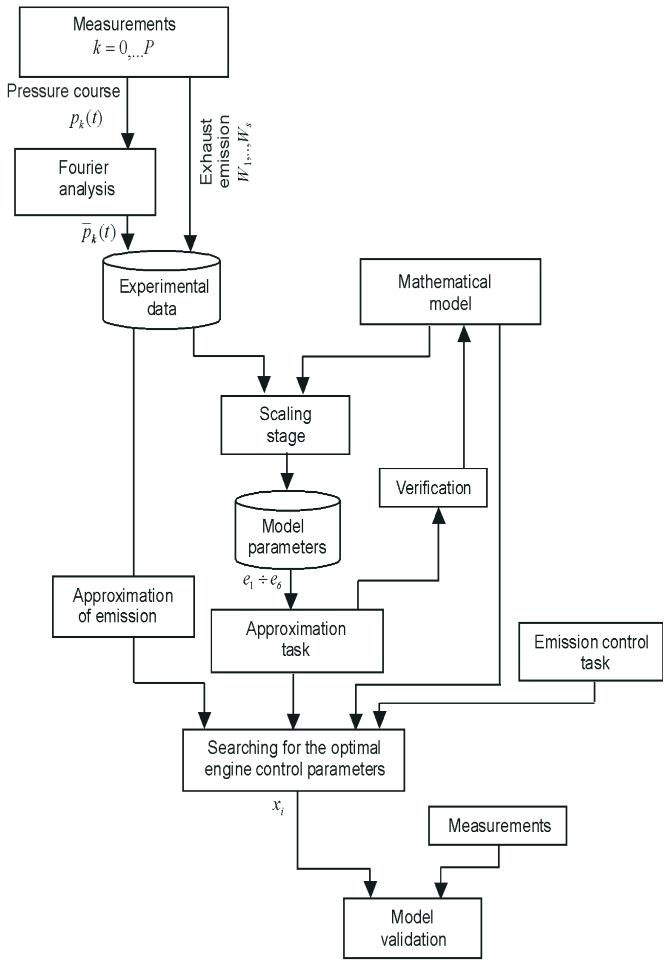

Fig. 1. General algorithm allowing formulation of the computational model of the working cycle of a CI engine and emission control study

Model calibration (for an extended set of model parameters) and new validation measurements were carried out for the same, as in paper [1], CI engine supercharged by a turbo compressor with intercooler, an electronically controlled direct injection unit with a distributing injection pump. The AVL instrumentation was used in the measurements carried out on eddy current dynamometer test stand. For high speed in-cylinder pressure and injector push tube load data the AVL Indimeter 619 was used with PC-based AVL acquisition software. The AVL GU 12S piezoelectric transducer was used in-cylinder pressure measurement and the AVL 364X precision optical encoder (0.2 crank angle resolution) for TDC (top dead centre) marking. The AVL QL 61D piezoelectric transducer was used for high speed in-line pressure. Fuel consumption was measured by the AVL 733S Dynamic Fuel Meter. The concentration of toxic components was measured by Pierburg modular instrumentation, which uses CLD, HFID and NDIR methods. The AVL 409P Smoke Meter was used for smoke. The engine set-up under investigation is presented in Figure 2.

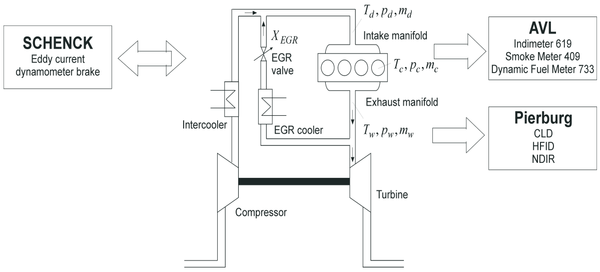

Fig. 2. Schematic layout of the experimental set-up (CLD – chemiluminescent detector, HFID – heated flame ionization detector, NDIR – non-dispersive infrared)

The operating conditions for which the experimental measurements were performed were chosen according to the rules for the test ESC [18]. Engine operating conditions in measurements are given in Table 1.

Table 1.

Engine operating conditions in measurements

	Crankshaft rotational speed [rpm]			
Load [Nm]	**1880**	**2610**	**3340**	**4070**
$M_{\max}$	143	163	137	129
0.75 $M_{\max}$	107	122	104	96
0.5 $M_{\max}$	72	82	69	64
0.25 $M_{\max}$	36	41	35	32

The following parameters were measured: pressure in the cylinder and in the fuel pipe, power, torque, specific fuel consumption, temperature and pressure in the engine turbo charge system. The measurements were performed for different engine load and possible recirculation degrees in various operating conditions. The fuel dose was not divided into the pre- and main doses. The value of standard injection advanced angle was used in each engine operating point. Moreover, measurements were also performed for the value standard injection advanced angle increased and decreased by five degree.

2. Mathematical model of the working cycle

This study uses the model presented as the result of earlier works [1]. The assumptions for the model concerned a four-stroke compression ignition engine featuring a turbocharger with intercooler and exhaust gas recirculation (EGR) with cooler, which both introduce feedback loops from the exhaust to the intake manifold. This leads to the substantial increase in calibration effort. In the model two main elements, the engine cylinder and the turbocharger with EGR system, were distinguished. Physical processes during intake, compression, combustion, decompression and exhaust in the cylinder were described on the basis of the following assumptions:

– air with exhaust gases, considered as a semi–ideal gas, is the medium in the intake-exhaust system and cylinder,
– specific heat of the medium depends on the temperature and species,
– thermodynamic processes within the engine were described on the basis of the first law of thermodynamics for the open system,
– losses of mass due to a leakage between a piston with rings and the cylinder lining were left out,
– flows through inlet and exhaust valves were described as isentropic flows trough a converged nozzle,
– the intake to the cylinder is accomplished by the intake manifold with the turbocharger and EGR system; at the inlet valves there are parameters described by the experimental maps of the turbocharger.

The outflow from the cylinder to the exhaust manifold occurs at parameters which are also described by the experimental maps of the turbocharger. Differences between static and dynamic pressures and temperatures were omitted due to low gas velocities.

– heat loss through cylinder walls was described by the Newton convection formula. Heat loss through manifold walls, pressure drop across the EGR and intercooler systems, and accumulated mass in the EGR system were left out,

– the combustion process was described by the Vibe function. The input to the model was the injected fuel mass.

These assumptions show that the model used in this study is of limited complexity only, which is justified by its purpose of controlling CI engine exhaust emission under steady-state conditions. In this paper, these conditions are described by the vector $\boldsymbol{X}$ of six basic engine control parameters $x_1 \div x_6$: crankshaft rotational speed, injected fuel mass, injection advance angle, temperature and pressure of the medium in the intake manifold and degree of exhaust gas recirculation. Contrary to the work presented in [1], this study uses an extended number of model parameters which characterise the model: total combustion duration, start of combustion, Vibe constant, discharge coefficients for inlet and exhaust valves and heat exchange parameters in the Hohenberg formula. These parameters are denoted as model parameters and have to be known for each set of control engine parameters. Allowable values of the control and model parameters are presented in Table 2. A procedure similar to the scaling procedure presented in paper [1] was applied, i.e. the appropriate values of model parameters would be made known by using the optimization methods.

Table 2.

Engine control parameters and model parameters

Notation		Parameter	Unit	Range
Engine control parameters				
x_1	n	crankshaft rotational speed	[rpm]	$1800 \div 4100$
x_2	B_0	injected fuel mass	[kg]	$10^{-5} \div 3 \cdot 10^{-5}$
x_3	φ_w	injection advance angle	[^{o}CA]	$-20 \div 0$
x_4	p_d	intake manifold pressure	[Pa]	$0.1 \cdot 10^6 \div 0.16 \cdot 10^6$
x_5	T_d	temperature in the intake manifold	[K]	$320 \div 370$
x_6	X_{EGR}	degree of exhaust gas recirculation	[%]	$0 \div 12$
Model parameters				
e_1	$\Delta\varphi_s$	total combustion duration	[^{o}CA]	$10 \div 100$
e_2	φ_z	start of combustion	[^{o}CA]	$-15 \div 5$
e_3	m_v	Vibe constant	[–]	$0.1 \div 1$
e_4	k_h	coefficient in the Hohenberg formula	[–]	$65 \div 260$
e_5	μ_d	inlet valve discharge coefficient	[–]	$0.1 \div 1$
e_6	μ_w	exhaust valve discharge coefficient	[–]	$0.1 \div 1$

Equations of the mathematical model can be symbolically written as [1]:

$$M_i\left[\boldsymbol{X},\boldsymbol{E},p,V,m,T\right]=0 \quad \text{for} \quad i=1,...,l \tag{1}$$

where:

M_i – differential operator or function,

l – number of equations,

$\boldsymbol{X}=[x_1...x_6]^T$ – vector of control parameters,

$\boldsymbol{E}=[e_1...e_6]^T$ – vector of model parameters.

The discrete model parameters obtained by a scaling (calibration) procedure were approximated by power functions:

$$f_s\left(x_1,...,x_6\right)=\delta_0^{(s)}x_1^{\delta_1^{(s)}}\cdot...\cdot x_j^{\delta_j^{(s)}}\cdot...\cdot x_6^{\delta_6^{(s)}}, \tag{2}$$

using the least squares method [19]. The same approximation method (2) was used for approximation of the total emission of CO, HC, NO_x and smoke (D). It was shown in the paper [1] that this kind of approximation enables calculation of emission and the values of model parameters for all possible values of engine control parameters with an acceptable accuracy.

2.1. Model verification

In order to verify the calibrated model with an extended number of model parameters, some additional experimental measurements were carried out. Values of control parameters different from those taken in previous measurements were taken, and all model parameters were calculated according to the approximation functions (2). Figure 3 shows the relation between mean indicated pressure in the cylinder, mass of the medium in the cylinder, maximum pressure in the cylinder and thermal efficiency obtained by our model and from measurements. Figure 4 presents a comparison between the results of measurements and modelling for exhaust gas components analysed.

Additionally, four error metrics were calculated:

– maximum relative error:

$$\mathrm{MRE}=\max\frac{w_{\exp}-w}{w_{\exp}}, \tag{3}$$

– mean relative error:

$$\mathrm{MNRE}=\overline{\left(\frac{w_{\exp}-w}{w_{\exp}}\right)}, \tag{4}$$

– normalized mean square error:

$$\mathrm{NMSE}=\frac{\overline{\left(w_{\exp}-w\right)^2}}{\bar{w}_{\exp}\bar{w}}, \tag{5}$$

– fractional bias:

$$\mathrm{FB} = \frac{\left(\bar{w}_{\exp} - \bar{w}\right)}{0.5\left(\bar{w}_{\exp} + \bar{w}\right)}, \tag{6}$$

where $w_{\exp}, w$ are experimental and measured values respectively, over-bars denote the average value.

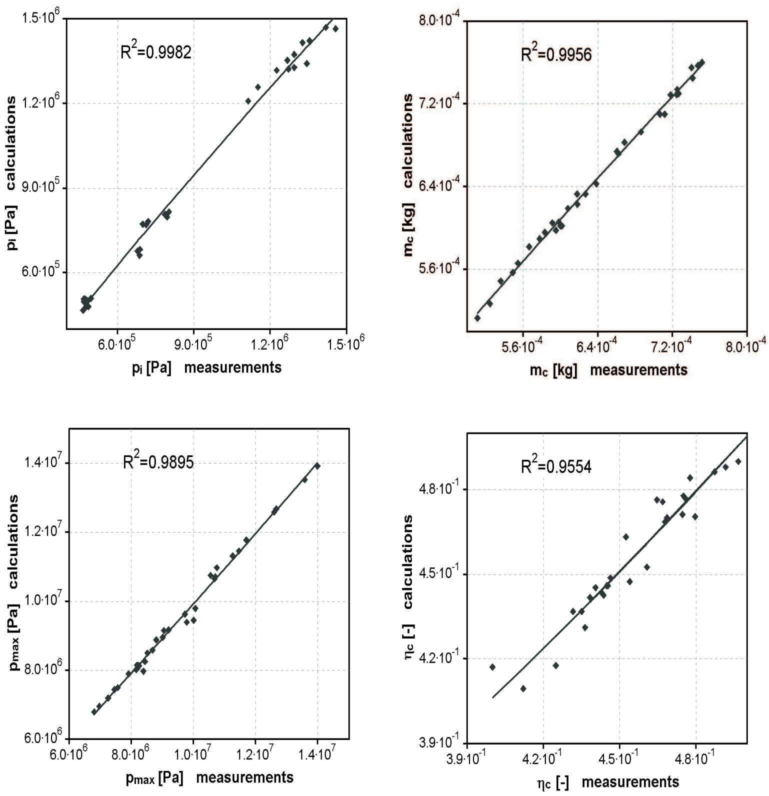

Fig. 3. Comparison of modelled and measured mean indicated pressure in the cylinder, mass of the medium in the cylinder, maximum pressure in the cylinder and thermal efficiency

Values of these errors are presented in Table 3. Almost in each case, low values of normalized mean square error were achieved. The higher NMSE value was obtained for smoke. Maximum and mean relative errors for mean indicated pressure, mass of the medium in the cylinder, maximum pressure in the cylinder and thermal efficiency were less than 0.11 and 0.05 respectively. Comparable values of MRE and MNRE for emission of NO_x and HC were obtained as well. Comparison of all metrics shows less accuracy of modelling for emission of CO and smoke (D). Additionally, analysis of fractional bias leads to the conclusion that no systematic errors occurred. The values of the error metrics show an acceptable accuracy of modelling using the calibrated model.

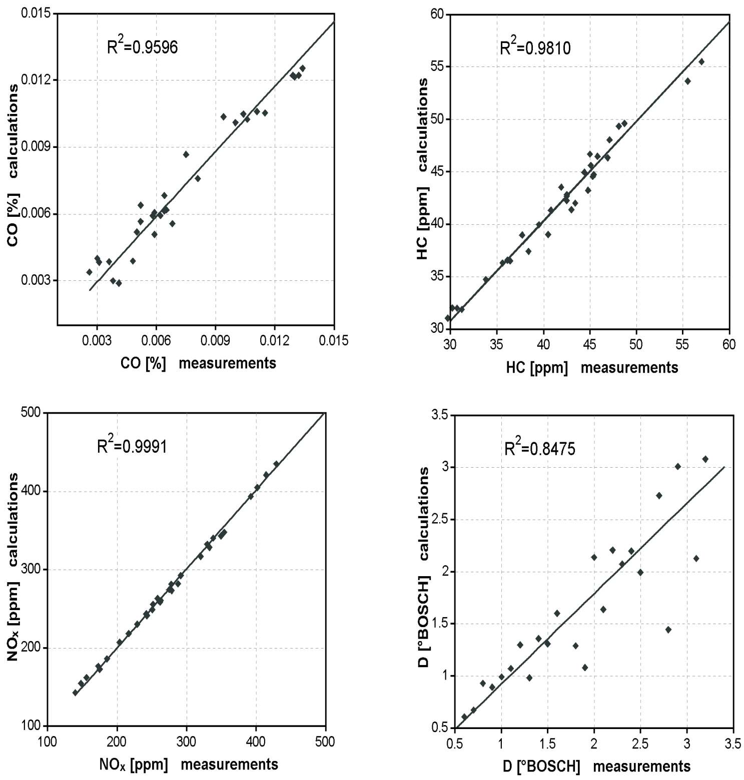

Fig. 4. Comparison of modelled and measured concentration of CO, HC, NO_x and smoke (D)

Table 3.

Values of modelling errors relative to measurement results

	MRE	**MNRE**	**NMSE**	**FB**
p_i	0.1045	0.0438	0.0032	0.0407
m_c	0.0277	0.0126	0.0002	0.0121
$p_{\max}$	0.0561	0.0118	0.0003	–0.0069
η_c	0.1045	0.0390	0.0023	0.0105
CO	0.336	0.1179	0.0107	–0.020
HC	0.0602	0.0234	0.0006	0.0048
NO_x	0.0432	0.0132	0.0002	0.0033
Smoke (D)	0.4842	0.1243	0.0628	–0.1038

3. Formulation of the emission control task

The presented model ensures that the values of model parameters $e_1 \div e_6$ are determined on the basis of experimental measurements. The model, which includes thermodynamic processes, enables formulation of the emission optimization task. The result of this optimization would be a choice of control parameters $x_1 \div x_6$ that would ensure reduction or minimization of emission of exhaust gas components. The components of vector $\boldsymbol{X}$ have to fulfil the following conditions:

$$x_{i\,\min} \leq x_i \leq x_{i\,\max} \quad \text{for} \quad i = 1, ..., 6, \tag{7}$$

where $x_{i\,\min}, x_{i\,\max}$ are maximum and minimum possible values of parameter x_i respectively, according to the range of parameters presented in Table 1.

Emission of the i-th exhaust gas component is denoted by W_i, the i-th function obtained by integration of the model equations by U_i as components of vector $\boldsymbol{U}$ for $\varphi \in \langle 0, 4\pi \rangle$:

$$\boldsymbol{U} = \left[p_c(\varphi), m_c(\varphi), T_c(\varphi), V_c(\varphi), \frac{dp_c}{d\varphi}, \frac{dm_c}{d\varphi}, \frac{dT_c}{d\varphi}, \eta_c(\varphi), p_i(\varphi) \right]^T, \tag{8}$$

where

$$U_8(\varphi) = \eta_c = \frac{\int\limits_V p_c\, dV}{B_0 W}, \tag{9}$$

$$U_9(\varphi) = p_i = \frac{\int\limits_V p_c\, dV}{V_c}. \tag{10}$$

Additionally, the notation $L_i[U]$ is used for values of functionals of the components of vector $\boldsymbol{U}$, i.e.

$$L_1[U] = \int\limits_V p_c\, dV = \int\limits_0^{4\pi} p_c \frac{dV}{d\varphi} \cdot \frac{d\varphi}{dt} dt, \tag{11}$$

$$L_2[U] = \max_{0 \leq \varphi \leq 4\pi} \{p_c(\varphi)\}, \tag{12}$$

$$L_3[U] = \max_{0 \leq \varphi \leq 4\pi} \left\{ \frac{dp_c}{d\varphi} \right\}. \tag{13}$$

According to the definitions given above, the optimization task is carried out in order to find the minimum of the expression:

$$\Omega\,(\mathbf{X}) = \sum_{i=1}^{s} C_i^w \cdot W_i + \sum_{i=1}^{q} C_i^L \cdot L_i\,[U], \tag{14}$$

where C_i^W, C_i^L are coefficients. The conditions for design variables are as follows:

$$W_{i\,\min} \leq W_i \leq W_{i\,\max} \quad \text{for} \quad i = 1, ..., s, \tag{15}$$

$$L_{i\,\min} \leq L_i\,[U] \leq L_{i\,\max} \quad \text{for} \quad i = 1, ..., q. \tag{16}$$

where $W_{i\,\min}, L_{i\,\min}, W_{i\,\max}, L_{i\,\max}$ are minimum and maximum possible values of design variables W_i,L_i respectively.

Calculation of the objective function Ω and the components of a vector $\boldsymbol{U}$ at each step of the optimization procedure requires integration of model equations.

The initial values of control parameters $x_1^{beg}, ..., x_6^{beg}$ have to be known in order to solve the optimization task. By integrating the model equations using vector $\boldsymbol{X}^{beg}$ one can calculate the initial values of:

$$L_i^{beg} = L_i\left[U\left[\mathbf{X}^{beg}\right]\right] \quad \text{for} \quad i = 1, ..., q. \tag{17}$$

The initial emission of all gas components is obtained on the basis of $\mathbf{X}^{beg}$ by using approximation function (2):

$$W_i^{beg} = W_i\left[\mathbf{X}^{beg}\right] = f_s\left(\mathbf{X}^{beg}\right) \quad \text{for} \quad i = 1, ..., s. \tag{18}$$

Using the initial values of $W_i, L_i\,[U]$ in conditions (15–16), ensures that additional conditions, e.g. limit of maximum pressure in the cylinder or exhaust emission, will be fulfilled.

The optimization task for minimization of NO_x emission is presented below. Additional conditions used in the optimization task were formulated in order to:

– control emission of CO, HC and smoke (D),
– maintain the value of mean effective pressure in the cylinder,
– minimize decrease of thermal efficiency,
– control the maximum pressure in the cylinder
– control the maximum temperature in the cylinder.

These conditions mean that in equation (14) for:

$$W = [W_1 = NO_x, W_2 = CO, W_3 = HC, W_4 = D]\,, \tag{19}$$

the following dependencies are used:

$$C_1^w = \frac{1}{C_1^{w,beg}}, \tag{20}$$

$$C_2^w = C_3^w = C_4^w = 0, \tag{21}$$

$$C_i^L = 0, \tag{22}$$

$$L_1 [U] = p_i, \tag{23}$$

$$L_2 [U] = \eta_c, \tag{24}$$

$$L_3 [U] = p_{\max}, \tag{25}$$

$$L_4 [U] = T_{\max}, \tag{26}$$

where $C_1^{w,beg}$ is emission of NO_x for $\mathbf{X} = \mathbf{X}^{beg}$.

Additionally, the conditions are taken into account by:

$$W_i \leq k_i^w \cdot W_i^{beg} \quad \text{for} \quad i = 2, 3, 4, \tag{27}$$

where $k_2^w = 3$, $k_3^w = 2$, $k_4^w = 2$,
and

$$L_i [U] \geq k_i^l \cdot L_i \left[U \left[\mathbf{X}^{beg}\right]\right] \quad \text{for} \quad i = 1, 2, \tag{28}$$

$$L_i [U] \leq k_i^l \cdot L_i \left[U \left[\mathbf{X}^{beg}\right]\right] \quad \text{for} \quad i = 3, 4, \tag{29}$$

where k_1^l =1.0, $k_2^l = 0.9$, $k_3^l = 1.1$, k_4^l =1.1.

Conditions (27–29) mean that emission of CO, HC and smoke (D) cannot be larger than 300%, 200%, 200% respectively, of those for $\mathbf{X}^{beg}$, and the value of mean effective pressure must be the same as the start value, thermal efficiency must not be less than 90% of the start value, maximum pressure in the cylinder and maximum temperature cannot be higher than 110% of initial values.

The optimization procedure with additional conditions of constant values for control engine parameters x_1 and x_6 was carried out for different engine operating conditions. The calculated optimal engine control parameters $\mathbf{X}^{opt}$ are presented in Table 4.

Table 4.

Initial $\mathbf{X}^{beg}$ and obtained optimal $\mathbf{X}^{opt}$ values of control engine parameters

Load	**Engine control parameters**	Crankshaft rotational speed [rpm]					
		1884		**2612**		**3343**	
		$\mathbf{X}^{beg}$	$\mathbf{X}^{opt}$	$\mathbf{X}^{beg}$	$\mathbf{X}^{opt}$	$\mathbf{X}^{beg}$	$\mathbf{X}^{opt}$
0.25 M_{max}	n[rpm]	1884	1884	2612	2612	3343	3343
	B_0[kg]	$8.8{\cdot}10^{-6}$	$9.3{\cdot}10^{-6}$	$9.7{\cdot}10^{-6}$	$10.7{\cdot}10^{-6}$	$10.2{\cdot}10^{-6}$	$10.7{\cdot}10^{-6}$
	φ_w[°CA]	–8	–4.1	–10.5	–0.5	–13	–3
	X_{EGR}[%]	0	6	0	8	0	8
	p_d[Pa]	$1.16{\cdot}10^{6}$	$1.16{\cdot}10^{6}$	$1.36{\cdot}10^{6}$	$1.44{\cdot}10^{6}$	$1.42{\cdot}10^{6}$	$1.54{\cdot}10^{6}$
	T_d[K]	334	334	332	332	331	331
0.5 M_{max}	n[rpm]	1884	1884	2612	2612	3343	3343
	B_0[kg]	$13.8{\cdot}10^{-6}$	$14.6{\cdot}10^{-6}$	$15.9{\cdot}10^{-6}$	$16.8{\cdot}10^{-6}$	$14.9{\cdot}10^{-6}$	$15.6{\cdot}10^{-6}$
	φ_w[°CA]	–9	–4.3	–12	–5.5	–13.5	–3.5
	X_{EGR}[%]	0	6	0	8	0	8
	p_d[Pa]	$1.28{\cdot}10^{6}$	$1.35{\cdot}10^{6}$	$1.46{\cdot}10^{6}$	$1.65{\cdot}10^{6}$	$1.47{\cdot}10^{6}$	$1.63{\cdot}10^{6}$
	T_d[K]	334	334	332	332	331	331
0.75 M_{max}	n[rpm]	1884	1884	2612	2612	3343	3343
	B_0[kg]	$19{\cdot}10^{-6}$	$20{\cdot}10^{-6}$	$21.7{\cdot}10^{-6}$	$21.7{\cdot}10^{-6}$	$20.9{\cdot}10^{-6}$	$20.9{\cdot}10^{-6}$
	φ_w[°CA]	-12	-5.6	-14	-14	-13	-13
	X_{EGR}[%]	0	6	0	8	0	8
	p_d[Pa]	$1.39{\cdot}10^{6}$	$1.49{\cdot}10^{6}$	$1.52{\cdot}10^{6}$	$1.75{\cdot}10^{6}$	$1.52{\cdot}10^{6}$	$1.75{\cdot}10^{6}$
	T_d[K]	334	334	334	334	332	332

The emission and values of additional parameters taken into account in optimization as initial (*beg*) for $\mathbf{X}^{beg}$ and those obtained after optimization (*opt*) for $\mathbf{X}^{opt}$ are presented in Table 5. The values of design parameters presented in Table 5 show that for optimization conditions (27–29) a significant reduction of emission of NO_x was obtained (in presented cases up to 50%).

The optimal engine control parameters $\mathbf{X}^{opt}$ were used in new measurements in order to ascertain the correctness and accuracy of the method. The calculated emission and other parameters from Table 5 were compared with the data from measurements. The comparison of emissions of exhaust gas components obtained as a result of optimization according to the data from validation measurements is presented in Figure 5. Although the calculated emission of some exhaust gas components in several cases is lower than the real emission, real emission of those components is still below their permissible levels taken into account in optimization task.

Table 5.

Comparison between initial and obtained optimal values of W_i and $L_i\,[U]$

Load	$\mathbf{W}_i$ and $L_i\,[U]$	**Crankshaft rotational speed [rpm]**					
		1884		**2612**		**3343**	
		beg	**opt**	**beg**	**opt**	**beg**	**opt**
0.25 M_{max}	CO [%]	0.015	0.040	0.016	0.027	0.007	0.010
	HC [ppm]	72	82	55	67	45	44
	NO_x [ppm]	272	184	280	143	268	124
	D [°BOSCH]	0.4	0.4	0.5	0.8	0.4	0.6
	p_i[Pa]	$0.44{\cdot}10^6$	$0.44{\cdot}10^6$	$0.49{\cdot}10^6$	$0.49{\cdot}10^6$	$0.51{\cdot}10^6$	$0.51{\cdot}10^6$
	η_c[–]	0.473	0.449	0.490	0.456	0.486	0.467
	$p_{\max}$[Pa]	$7.35{\cdot}10^6$	$6.07{\cdot}10^6$	$8.49{\cdot}10^6$	$7.53{\cdot}10^6$	$8.97{\cdot}10^6$	$8.03{\cdot}10^6$
	$T_{\max}$[K]	1490	1580	1485	1412	1500	1380
0.5 M_{max}	CO [%]	0.008	0.010	0.012	0.014	0.005	0.013
	HC [ppm]	49	47	44	49	37	52
	NO_x [ppm]	513	318	522	296	436	211
	D [°BOSCH]	0.3	0.6	0.4	0.7	0.5	0.8
	p_i[Pa]	$0.69{\cdot}10^6$	$0.69{\cdot}10^6$	$0.82{\cdot}10^6$	$0.82{\cdot}10^6$	$0.76{\cdot}10^6$	$0.76{\cdot}10^6$
	η_c[–]	0.486	0.462	0.497	0.472	0.492	0.443
	$p_{\max}$[Pa]	$8.95{\cdot}10^6$	$7.29{\cdot}10^6$	$10.82{\cdot}10^6$	$8.69{\cdot}10^6$	$10.34{\cdot}10^6$	$8.49{\cdot}10^6$
	$T_{\max}$[K]	1682	1703	1690	1623	1673	1595
0.75 M_{max}	CO [%]	0.004	0.006	0.006	0.007	0.007	0.008
	HC [ppm]	45	44	39	42	36	36
	NO_x [ppm]	880	525	793	656	482	378
	D [°BOSCH]	0.3	0.5	0.3	0.4	0.8	0.9
	p_i[Pa]	$0.96{\cdot}10^6$	$0.96{\cdot}10^6$	$1.11{\cdot}10^6$	$1.11{\cdot}10^6$	$1.04{\cdot}10^6$	$1.04{\cdot}10^6$
	η_c[-]	0.492	0.477	0.492	0.493	0.471	0.479
	$p_{\max}$[Pa]	$11.26{\cdot}10^6$	$8.93{\cdot}10^6$	$12.57{\cdot}10^6$	$12.59{\cdot}10^6$	$10.69{\cdot}10^6$	$10.9{\cdot}10^6$
	$T_{\max}$[K]	1871	1909	1885	1910	1820	1805

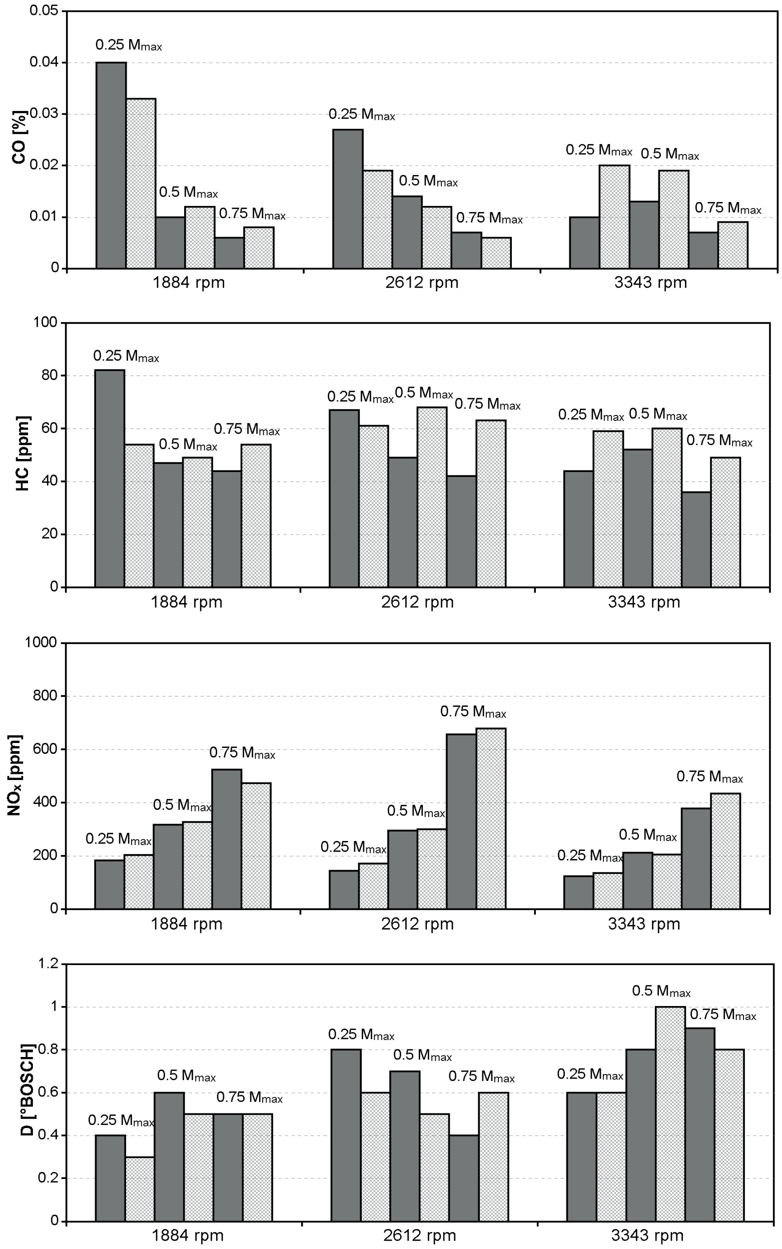

Fig. 5. Emissions of exhaust gas components as a result of the optimization procedure (dark grey) according to data from the validation experiment (light grey)

Comparison of values of mean effective pressure, thermal efficiency, maximum pressure and temperature obtained from optimization and validation measurements is presented in Table 6. The maximum relative percentage error of calculation is equal to 16.8%, but in many cases the errors are lower than ±6%. The highest errors occurred in the case of engine load equal to $0.25M_{\max}$.

Table 6.

Comparison between the values of $L_i\,[U]$ obtained from optimization and from validation measurements

Load	$L_i\,[U]$	**Crankshaft rotational speed [rpm]**								
		1884			**2612**			**3343**		
		opt	**exp**	**err. [%]**	**opt**	**exp**	**err. [%]**	**opt**	**exp**	**err. [%]**
0.25 $\boldsymbol{M}_{max}$	p_i[Pa]	$0.44\cdot10^6$	$0.4\cdot10^6$	**11.1**	$0.49\cdot10^6$	$0.47\cdot10^6$	**4.1**	$0.51\cdot10^6$	$0.46\cdot10^6$	**11.8**
	η_c[–]	0.449	0.434	**3.6**	0.456	0.450	**1.3**	0.467	0.400	**16.8**
	$p_{\max}$[Pa]	$6.07\cdot10^6$	$6.13\cdot10^6$	**–1.0**	$7.53\cdot10^6$	$7.4\cdot10^6$	**1.8**	$8.03\cdot10^6$	$8.4\cdot10^6$	**–4.4**
	$T_{\max}$[K]	1580	1409	**12.1**	1412	1492	**–5.4**	1380	1470	**–6.1**
0.5 $\boldsymbol{M}_{max}$	p_i[Pa]	$0.69\cdot10^6$	$0.67\cdot10^6$	**3.4**	$0.82\cdot10^6$	$0.77\cdot10^6$	**6.0**	$0.76\cdot10^6$	$0.72\cdot10^6$	**5.4**
	η_c[–]	0.462	0.454	**1.7**	0.472	0.453	**4.2**	0.443	0.417	**6.2**
	$p_{\max}$[Pa]	$7.29\cdot10^6$	$6.92\cdot10^6$	**5.4**	$8.69\cdot10^6$	$8.66\cdot10^6$	**0.4**	$8.49\cdot10^6$	$8.86\cdot10^6$	**–4.1**
	$T_{\max}$[K]	1703	1686	**1.0**	1623	1636	**–0.8**	1595	1643	**–2.9**
0.75 $\boldsymbol{M}_{max}$	p_i[Pa]	$0.96\cdot10^6$	$0.93\cdot10^6$	**3.8**	$1.11\cdot10^6$	$1.14\cdot10^6$	**–2.8**	$1.04\cdot10^6$	$0.99\cdot10^6$	**3.8**
	η_c[–]	0.477	0.482	**–1.1**	0.493	0.480	**2.7**	0.479	0.427	**12.2**
	$p_{\max}$[Pa]	$8.93\cdot10^6$	$8.49\cdot10^6$	**5.2**	$12.6\cdot10^6$	$12.4\cdot10^6$	**1.5**	$10.9\cdot10^6$	$10.5\cdot10^6$	**4.3**
	$T_{\max}$[K]	1909	1905	**0.2**	1910	1970	**–3.0**	1805	1799	**0.3**

Figures 6–8 present a comparison of pressure courses in the cylinder obtained from the model and from validation measurements for an optimal values of engine control parameters. It can be seen that there is an acceptable correlation of the pressure courses obtained from the model and those from validation measurements.

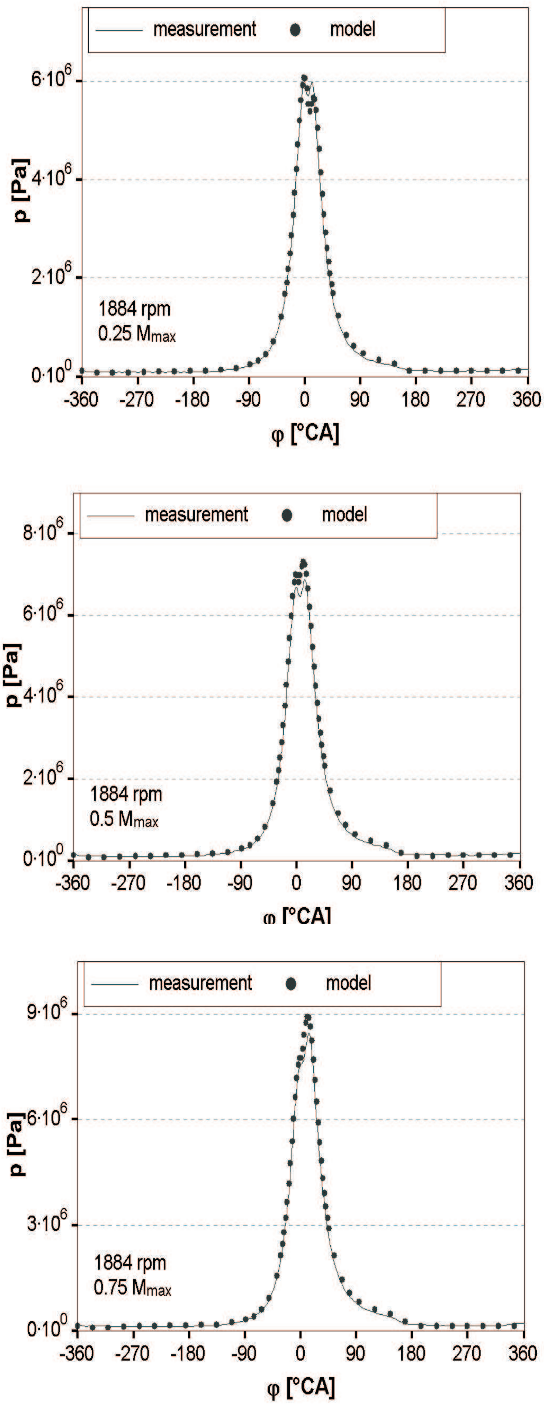

Fig. 6. Comparison of pressure courses of the medium in the cylinder for optimal engine control parameters obtained from the model (Table 6 data for crankshaft rotational speed equal to 1884 rpm) according to engine measurements

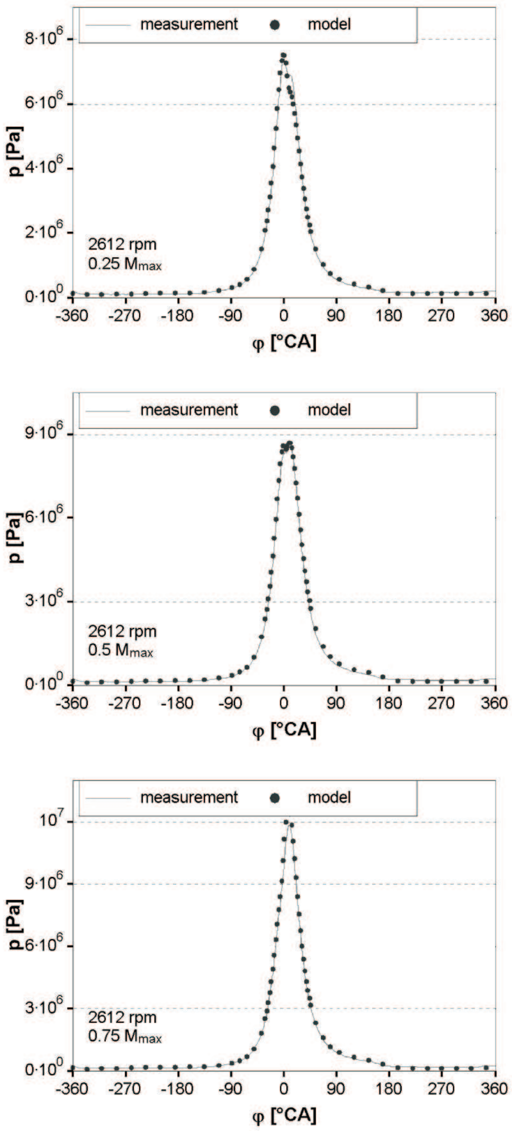

Fig. 7. Comparison of pressure courses of the medium in the cylinder for optimal engine control parameters obtained from the model (Table 6 data for crankshaft rotational speed equal to 2612 rpm) according to engine measurements

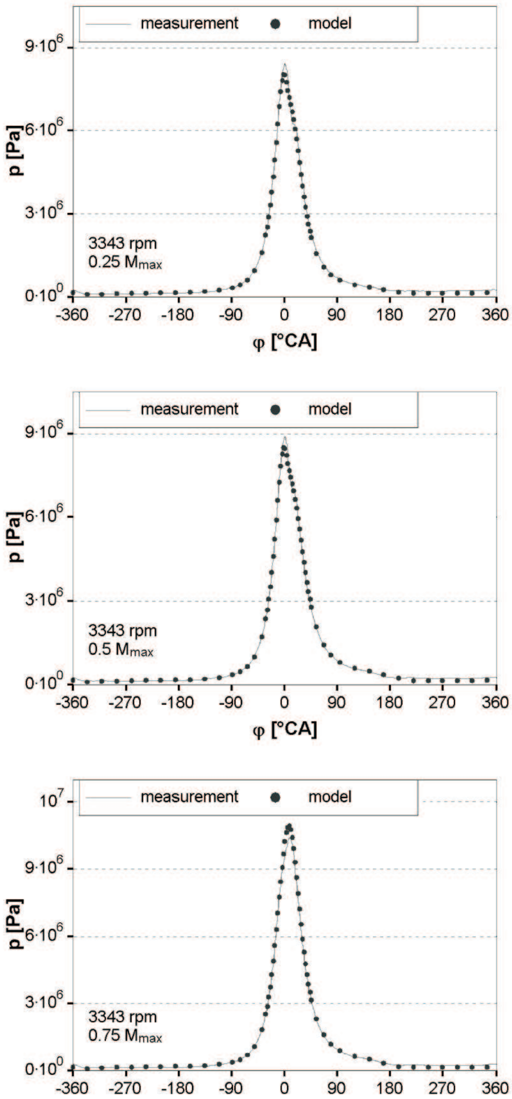

Fig. 8. Comparison of pressure courses of the medium in the cylinder for optimal engine control parameters obtained from the model (Table 6 data for crankshaft rotational speed equal to 3343 rpm) according to engine measurements

4. Conclusions

There are several advantages of using the semi-empirical model in the emission control task. The most important is its numerical effectiveness. In the paper, semi-empirical model was used in the optimization task formulated and carried out in order to minimize emission of nitrogen oxides. The validation of numerical calculations was performed using additional measurements. A good correspondence of model results with measurements was achieved, especially for nitrogen oxides. However, the accuracy of predicted emission for other exhaust gas components is not sufficient in a few cases. This could be the reason for local approximation errors that appear when using the power form of function (2). Taking into account the above restrictions, on the basis of validation, one can conclude that the semi-empirical model of the working cycle, apart from its simplicity, can ensure acceptable accuracy of results and can be used to control engine emissions under steady-state conditions.

The authors are aware of the effects of the simplifications made in formulating mathematical models. The chemical reactions during the combustion process, the local character of combustion and the wave processes in the intake and exhaust manifold were omitted. These problems can be investigated with the CFD model, but the computational time will be much longer than that in the semi-empirical model. Transient states of engine working, which also are currently important in engine control research, have not been incorporated in this study. In order to use our optimization method for more complicated models useful in transient problems further investigations will be necessary.

Manuscript received by Editorial Board, July 08, 2008;
final version, March 02, 2009.

REFERENCES

[1] Brzozowski K., Nowakowski J.: Application of optimization to scaling of the mathematical model of the working cycle of CI engine. The Archive of Mechanical Engineering, Vol. L II, pp. 21-39, 2005.
[2] Heywood J.B.: International Combustion Engine Fundamentals. Mc-Graw-Hill, New York, 1988.
[3] Watson N., Pilley A. D., Marzouk M.: A Combustion Correlation for Diesel Engine Simulation. SAE Paper 800029, 1980.
[4] Whitehouse N. D., Way R. J. B.: Simple Method for the Calculation of Heat Release Rates in Diesel Engines Based on the Fuel Injection Rate. SAE Paper 710134, 1971.
[5] Schubert C., Wimmer A., Chmela F.G.: Advanced Heat Transfer Model for CI Engines. SAE Paper 2005-01-0695, 2005.

[6] Vibe I. I.: Brennverlauf und Kreisprozess von Verbrennungsmotoren. VEB Verlag Technik Berlin, 1970.

[7] Friedrich I., Pucher H., Offer T.: Automatic Model Calibration for Engine-Process Simulation with Heat-Release Prediction. SAE Paper 2006-01-0655, 2006.

[8] Caton J.A.: Effects of the compression ratio on nitric oxide emissions for a spark ignition engine: results from a thermodynamic cycle simulation. International Journal of Engine Research, Vol. 4. No. 4, pp. 249-268, 2003.

[9] Heider G., Woschni G., Zeilinger K.: 2 – Zonen Rechenmodell zur Vorausrechnung der NO – Emission von Dieselmotoren. MTZ 11/1998.

[10] Belardini P., Bertoli C., Corsaro S., D'Ambra P.: Multidimensional Modeling of Advanced Diesel Combustion System by Parallel Chemistry. SAE Paper 2005-01-0201, 2005.

[11] Pariotis E. G., Hountalas D. T., Rakopoulos C. D.: Sensitivity Analysis of Multi-Zone Modeling for Combustion and Emissions Formation in Diesel Engines. SAE Paper 2006-01-1383, 2006.

[12] Arsie I., Di Genova F., Mogavero A., Pianese C., Rizzo G., Caraceni A., Cioffi P., Flauti G.: Multi-Zone Predictive Modeling of Common Rail Multi-Injection Diesel Engines. SAE Paper 2006-01-1384, 2006.

[13] Felsch C., Gauding M., Vanegas A., Won H., Luckhchoura V., Peters N. Hasse C., Ewald J.: Evaluation of Modeling Approaches for NOx Formation in a Common-Rail DI Diesel Engine within the Framework of Representative Interactive Flamelets (RIF). SAE Paper 2008-01-0971, 2008.

[14] Badami M., Millo F., D'Amato D.: Experimental investigation on soot and NO_x formation in a DI common rail diesel engine with pilot injection. SAE Paper 2001-01-0657, 2001.

[15] Han Z., Uludogan A., Hampson G. J., Reitz R. D.: Mechanism of soot and NO_x emission reduction using multiple-injection in a diesel engine. SAE Paper 960633, 1996.

[16] Hawley J. G., Wallace F. J., Cox A.: Reduction of Steady State NOx Levels from an Automotive Diesel Engine Using Optimised VGT/EGR Schedules. SAE Paper 1999-01-0835, 1999.

[17] Vitek O., Macek. J., Polasek M., Schmerbeck S., Kammerdiener T.: Comparison of Different External EGR Solutions. SAE Paper 2008-01-0206, 2008.

[18] Directive 1999/96/EC of the European Parliament and of the Council of 13 December 1999. Official Journal of the European Communities, 1999.

[19] Chapra S.C., Canale R. P.: Numerical methods for engineers. McGraw-Hill Higher Education. New York, 2002.

Zastosowanie metody optymalizacji do sterowania emisją z silnika o zapłonie samoczynnym w warunkach ustalonych

Streszczenie

W artykule do ograniczenia emisji w warunkach ustalonych wykorzystano pół-empiryczny model cyklu roboczego silnika ZS przedstawiony przez autorów we wcześniejszej pracy [1]. Sformułowano metodę optymalizacji umożliwiającą ustalenie wartości parametrów regulacyjnych silnika, dla których można uzyskać minimalizację emisji tlenków azotu. Zaproponowana metoda postępowania zapewnia ponadto właściwe parametry robocze, takie jak: średnie ciśnienie indykowane, sprawność cieplną oraz ogranicza maksymalne ciśnienie w cylindrze. Wyniki modelowania porównywane są z wynikami badań eksperymentalnych. Uzyskano akceptowalną dokładność modelu.